

NASA/TM—2007–215132



# Conceptual Trade Study of General Purpose Heat Source Powered Stirling Converter Configurations

*J.B. Turpin*

*Marshall Space Flight Center, Marshall Space Flight Center, Alabama*

---

*November 2007*

## The NASA STI Program...in Profile

Since its founding, NASA has been dedicated to the advancement of aeronautics and space science. The NASA Scientific and Technical Information (STI) Program Office plays a key part in helping NASA maintain this important role.

The NASA STI program operates under the auspices of the Agency Chief Information Officer. It collects, organizes, provides for archiving, and disseminates NASA's STI. The NASA STI program provides access to the NASA Aeronautics and Space Database and its public interface, the NASA Technical Report Server, thus providing one of the largest collections of aeronautical and space science STI in the world. Results are published in both non-NASA channels and by NASA in the NASA STI Report Series, which includes the following report types:

- **TECHNICAL PUBLICATION.** Reports of completed research or a major significant phase of research that present the results of NASA programs and include extensive data or theoretical analysis. Includes compilations of significant scientific and technical data and information deemed to be of continuing reference value. NASA's counterpart of peer-reviewed formal professional papers but has less stringent limitations on manuscript length and extent of graphic presentations.
- **TECHNICAL MEMORANDUM.** Scientific and technical findings that are preliminary or of specialized interest, e.g., quick release reports, working papers, and bibliographies that contain minimal annotation. Does not contain extensive analysis.
- **CONTRACTOR REPORT.** Scientific and technical findings by NASA-sponsored contractors and grantees.

- **CONFERENCE PUBLICATION.** Collected papers from scientific and technical conferences, symposia, seminars, or other meetings sponsored or cosponsored by NASA.
- **SPECIAL PUBLICATION.** Scientific, technical, or historical information from NASA programs, projects, and missions, often concerned with subjects having substantial public interest.
- **TECHNICAL TRANSLATION.** English-language translations of foreign scientific and technical material pertinent to NASA's mission.

Specialized services also include creating custom thesauri, building customized databases, and organizing and publishing research results.

For more information about the NASA STI program, see the following:

- Access the NASA STI program home page at <<http://www.sti.nasa.gov>>
- E-mail your question via the Internet to <[help@sti.nasa.gov](mailto:help@sti.nasa.gov)>
- Fax your question to the NASA STI Help Desk at 301-621-0134
- Phone the NASA STI Help Desk at 301-621-0390
- Write to:  
NASA STI Help Desk  
NASA Center for AeroSpace Information  
7115 Standard Drive  
Hanover, MD 21076-1320

NASA/TM—2007–215132



# **Conceptual Trade Study of General Purpose Heat Source Powered Stirling Converter Configurations**

*J.B. Turpin*

*Marshall Space Flight Center, Marshall Space Flight Center, Alabama*

National Aeronautics and  
Space Administration

Marshall Space Flight Center • MSFC, Alabama 35812

---

***November 2007***

## **TRADEMARKS**

Trade names and trademarks are used in this report for identification only. This usage does not constitute an official endorsement, either expressed or implied, by the National Aeronautics and Space Administration.

Available from:

NASA Center for AeroSpace Information  
7115 Standard Drive  
Hanover, MD 21076-1320  
301-621-0390

This report is also available in electronic form at  
<<https://www2.sti.nasa.gov>>

## EXECUTIVE SUMMARY

In support of the Marshall Space Flight Center's efforts to establish the capability to perform nonnuclear system level testing and integration of radioisotope power systems, a parametric study of general purpose heat source (GPHS) powered Stirling converter configurations was performed. The goal of this study was to gain insight into the physics of transferring power from the GPHS modules to the Stirling engine while accounting for waste heat removal and parasitic losses to the environment. Six GPHS stack configurations were analyzed at three different Stirling power levels. The thermal profile of the integrated GPHS modules (for each configuration) was calculated to determine maximum temperatures for comparison to allowable material limits. Temperature profiles for off-nominal power conditions were also assessed in order to better understand how power demands from the Stirling engine impact the performance of a given configuration. The study resulted in the following findings:

(1) It is important that the overall system be as efficient as possible (in a thermal sense) in order to achieve a high level of specific power. However, the more efficient the system, the more rapid the temperature increase within the stack for off-nominal power conditions. This could result in more complicated methods of achieving active heat rejection in the case of Stirling failure, which in turn, results in a lower specific power. In order to achieve the highest specific power number that provides confidence in creating a working system, a balance must be made between efficiency and heat rejection capabilities.

(2) It is important to minimize radiator area, and therefore, radiator weight, but not necessarily at the expense of running at an increased cold shoe temperature, that would reduce the overall Stirling efficiency. This reduction in Stirling efficiency would result in an increase in the number of GPHS modules in the system, thereby increasing system mass and reducing the system specific power.

(3) A method to remove excess power from the system at off-nominal operating conditions must be included in the design.



## TABLE OF CONTENTS

1. INTRODUCTION .....	1
2. OVERVIEW OF GENERAL PURPOSE HEAT SOURCE .....	3
2.1 Fuel Pellet .....	4
2.2 Clad Material .....	4
2.3 Graphite Impact Shell .....	4
2.4 CBCF Disk and Sleeve .....	4
2.5 Aeroshell .....	5
3. BACKGROUND .....	6
3.1 Previous Work .....	7
3.2 Description .....	7
3.3 Assumptions .....	9
3.4 Modeling Tools .....	10
4. APPROACH .....	11
4.1 Radiator Sizing .....	12
4.2 Nominal Analysis .....	12
4.3 Off-Nominal Analysis .....	18
5. FUTURE WORK .....	19
6. SUMMARY .....	20
APPENDIX A—RESULTS FOR ALL STUDY CASES .....	21
A.1 Study Case for 80 $W_e$ Configuration .....	21
A.2 Study Case for 250 $W_e$ Configuration 1 .....	22
A.3 Study Case for 250 $W_e$ Configuration 2 .....	22
A.4 Study Case for 500 $W_e$ Configuration 1 .....	24
A.5 Study Case for 500 $W_e$ Configuration 2 .....	24
A.6 Study Case for 500 $W_e$ Configuration 3 .....	26
REFERENCES .....	29

## LIST OF FIGURES

1.	Exploded view of GPHS module .....	3
2.	Three GPHS simulators stacked together inside a vacuum chamber at MSFC .....	6
3.	Example of a 250 $W_e$ stack configuration .....	8
4.	Example of an efficiency versus temperature ratio (hot shoe divided by cold shoe temperature) for a 35 $W_e$ Stirling converter .....	8
5.	The six stack configurations analyzed in the trade study: (a) 80 $W_e$ , (b) 250 $W_e$ configuration 1, (c) 250 $W_e$ configuration 2, (d) 500 $W_e$ configuration 1, (e) 500 $W_e$ configuration 2, and (f) 500 $W_e$ configuration 3. ....	11
6.	Flow chart representation of the steps taken to obtain the results presented in this study .....	13
7.	Two-dimensional model of heat conduction through aeroshell used to determine the conduction shape factor .....	14
8.	Example of Stirling interface temperature as a function of the effective emissivity .....	16
9.	Analysis results for the 250 $W_e$ configuration 1 .....	17
10.	Analysis results for the 80 $W_e$ configuration 1 .....	22
11.	Analysis results for the 250 $W_e$ configuration 1 .....	23
12.	Stirling interface temperature as a function of effective emissivity for the 250 $W_e$ configuration 2 .....	23
13.	Maximum GPHS module temperature and interface temperature as a function of power demanded by the Stirling for the 250 $W_e$ configuration 2 .....	24
14.	Analysis results for the 500 $W_e$ configuration 1 .....	25
15.	Stirling interface temperature as a function of effective emissivity for the 500 $W_e$ configuration 2 .....	25
16.	Maximum GPHS module temperature and interface temperature as a function of power demanded by the Stirling for the 500 $W_e$ configuration 2 .....	26



## LIST OF FIGURES (Continued)

17.	Stirling interface temperature as a function of effective emissivity for the 500 W <sub>e</sub> configuration 3 .....	27
18.	Maximum GPHS module temperature and interface temperature as a function of power demanded by the Stirling for the 500 W <sub>e</sub> configuration 3 .....	27

## LIST OF TABLES

1.	Summary of results for all pertinent parameters for the six cases that were considered .....	21
----	--	----

## LIST OF ACRONYMS AND SYMBOLS

$^{238}\text{PuO}_2$	238 plutonium dioxide
CBCF	carbon-bonded carbon fiber
FWPF	fine weave pierced fabric
GIS	graphite impact shell
GPHS	general purpose heat source
GRC	Glenn Research Center
MLI	multilayer insulation
MSFC	Marshall Space Flight Center
RPS	radioisotope power system
SRG	Stirling radioscopic generator
TM	Technical Memorandum

## NOMENCLATURE

$A$	heat transfer area (m <sup>2</sup> )
$A_{\text{radiator}}$	radiator area (m <sup>2</sup> )
$F_{\text{gphs}}$	radiation shape factor from GPHS to insulation
$k$	thermal conductivity (W/m-K)
$n$	number of layers of insulation
$\dot{Q}$	thermal power (W)
$\dot{Q}_{\text{conducted}}$	thermal power conducted into or out of GPHS modules or the interface plate (W)
$\dot{Q}_{\text{generated}}$	thermal power generated by GPHS modules (W)
$\dot{Q}_{\text{radiation}}$	thermal power lost due to radiation (W)
$\dot{Q}_{\text{radiator}}$	thermal power delivered to space from the radiator (W)
$\dot{Q}_{\text{Stirling}}$	thermal power delivered to the Stirling (W)
$\dot{Q}_{\text{thermal}}$	thermal power generated by the GPHS modules (W)
$S_{\text{conduction}}$	conduction shape factor (w/k)
$T$	temperature
$T_{\text{cold shoe}}$	Stirling cold shoe temperature (K)
$T_{\text{gphs}}$	GPHS average temperature (K)
$T_{\text{inf}}$	temperature of the area surrounding the system (K)
$T_{\text{radiator}}$	bulk radiator temperature
$T_{\text{space}}$	bulk radiator temperature
$\dot{W}_{\text{eStirling}}$	electrical power generated by the Stirling converter

## NOMENCLATURE (Continued)

$\varepsilon$	emissivity
$\varepsilon_{\text{effective}}$	effective emissivity
$\varepsilon_{\text{gphs}}$	GPHS emissivity
$\varepsilon_s$	radiation insulation emissivity
$\eta_{\text{Stirling}}$	Stirling efficiency
$\sigma$	Stefan-Boltzmann constant ( $5.669 \times 10^{-08} \text{ W/m}^2\text{-K}^4$ )

## TECHNICAL MEMORANDUM

# CONCEPTUAL TRADE STUDY OF GENERAL PURPOSE HEAT SOURCE POWERED STIRLING CONVERTER CONFIGURATIONS

## 1. INTRODUCTION

NASA Marshall Space Flight Center (MSFC) has a history of successfully testing simulated fission reactor concepts.<sup>1</sup> To simulate the heat from fission for these concepts, electrical resistance heaters are employed. This approach uses electrical heating elements of various materials, sizes, and shapes strategically placed inside a mockup of a reactor core to obtain the appropriate dynamic power profile of the reactor. With this technique, nonnuclear system level integration and thermal hydraulic testing can be performed for a complete fission-based space nuclear power system. Due to the success of the fission reactor simulation work, expansion of this methodology to incorporate radioisotope power systems (RPSs) was initiated.

Currently, MSFC is fabricating its first generation of electrically powered simulators for RPS. The primary goal of this effort is to stack these simulators in multiple configurations and perform non-nuclear systems level integration and testing for a variety of RPS concepts. In RPSs, naturally decaying <sup>238</sup>plutonium dioxide (<sup>238</sup>PuO<sub>2</sub>) is one of several components that make up a general purpose heat source (GPHS) module. (See fig. 1 in sec. 2.) Heat is generated within the GPHS by the <sup>238</sup>PuO<sub>2</sub> and converted to electrical power through either passive or active means. Because of their reliability, thermoelectrics coupled to GPHS modules are the predominate passive conversion technology used today for space missions. This process uses a temperature difference between two dissimilar metals to produce electrical power. Currently, thermoelectrics are only 4 to 6 percent efficient (the conversion of thermal to electrical power) with research aiming for an efficiency of 10 to 12 percent.<sup>2</sup> If specific power is defined as generated electrical power divided by the mass of the overall power system, then a major goal of the RPS system is to increase specific power. More efficient active power conversion technologies are also being studied. Specifically, it has been shown that a Stirling engine coupled with a linear alternator (a Stirling converter) has the capability to reach a 28 to 36 percent efficiency.<sup>3</sup>

One of the challenges accompanying the use of a Stirling converter is to effectively transfer the thermal power generated from a set of GPHS modules to the Stirling's hot shoe in a manner that provides overall system efficiency while not exceeding the operating temperature limit ( $\approx 1,300$  °C) of any of the GPHS modules.

A second challenge is the capability of the system to reject heat in the event of a Stirling converter failure. If the Stirling removes less power from the GPHS modules during a transient or failure and the system does not have a method to dissipate that power, the GPHS module temperatures will

increase, seeking a new equilibrium condition with the potential for a catastrophic system failure should the module's upper temperature limit be exceeded.

To understand these challenges and to investigate potential configurations prior to testing, a conceptual trade study was performed and is documented in this Technical Memorandum (TM). The study examined six GPHS stack configurations with a range of Stirling converter power levels; specifically one 80  $W_e$ , two 250  $W_e$ , and three 500  $W_e$  configurations. The overall goals of the study were: (1) to gain an understanding, from a systems perspective, of which configurations would not violate GPHS module temperature limits, and (2) to understand how a reduction in power demanded by the Stirling affects the increase in average temperature of the GPHS modules. This provides insight into the consequence of stacking geometry with respect to the sensitivity of the GPHS module temperature and Stirling power demands.

## 2. OVERVIEW OF GENERAL PURPOSE HEAT SOURCE

The following discussion of the GPHS is taken from reference 3. Current RPSs consist of stacked general purpose heat source modules as illustrated in figure 1.

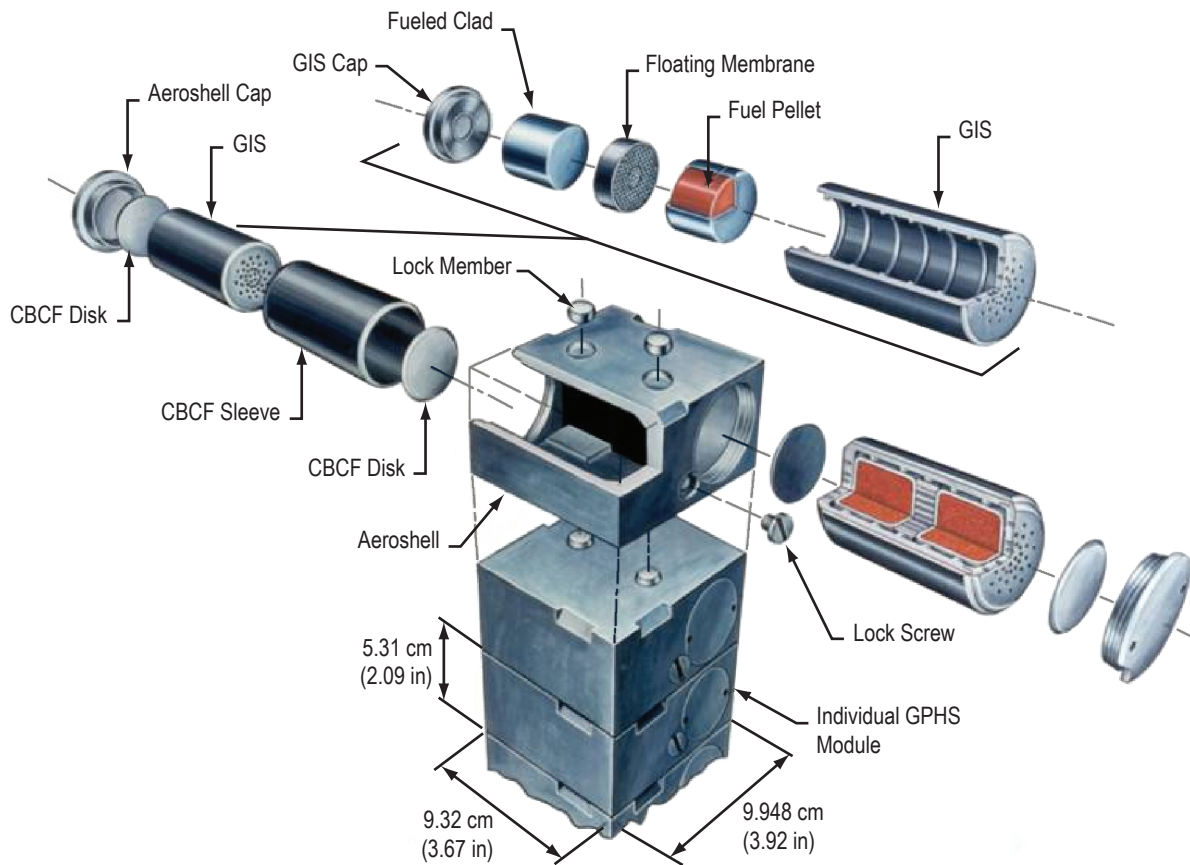


Figure 1. Exploded view of GPHS module.

The GPHS module is a block-shaped hexahedron with overall dimensions of 9.317 cm × 9.718 cm × 5.308 cm and a mass of ≈1.45 kg. Each module contains four iridium clad fuel pellets, two graphite impact shells, two thermal insulation sleeves, and an outer aeroshell. Initially, each block generates  $250 \pm 6$  W of thermal energy. The components of each module are illustrated in figure 1. The major components are described in the following subsections.

## 2.1 Fuel Pellet

Each GPHS module contains four radioisotope fuel pellets. The solid ceramic pellets are cylindrically shaped with an average diameter of  $2.753 \pm 0.025$  cm and an average length of  $2.756 \pm 0.038$  cm. The fuel material is an isotopic mixture of plutonium in the form of the dioxide,  $\text{PuO}_2$ . Each pellet contains an initial thermal inventory of  $62.5 \pm 1.5$  W that corresponds to  $152.4 \pm 3.7$  g of  $\text{PuO}_2$  per pellet.

## 2.2 Clad Material

The clad material's primary function is to prevent the release of radioactive material under all anticipated operating and accident conditions. Such conditions include ground transportation and handling, launch operations, ascent and orbital insertion, on-orbit operations, and reentry, impact, and post impact environmental behavior. In order to perform its intended function, two primary technical objectives must be satisfied: (1) the clad must be chemically compatible with the fuel material and the surrounding graphite impact shell (GIS) in all anticipated environments, and (2) the clad must be resistant to long-term air oxidation at elevated temperatures after surviving reentry and Earth impact. The clad material chosen for use in the GPHS is the iridium alloy, DOP-26 Ir, developed by Oak Ridge National Laboratories. This alloy was already known to be compatible with  $\text{PuO}_2$  and the GIS, and it had the best chance of meeting the second technical objective. Meeting the second objective was difficult due to temperature constraints imposed on the clad in order for it to retain adequate ductility to survive Earth impact. The clad surrounds the fuel pellet with a minimum thickness of 0.0559 cm. At one end of the fueled clad is a vent hole with a diameter of 0.04445 cm and a vent hole filter subassembly that allows the helium gas to escape but prevents the release of particles from inside the fuel pellet.

## 2.3 Graphite Impact Shell

As shown in figure 1, there are two GISs per GPHS module. Each GIS contains two iridium clad fuel pellets separated by a floating membrane. The GIS has a threaded end cap to secure its contents. The GIS, the floating membrane, and the end cap are all constructed of fine weave pierced fabric (FWPF) graphite. FWPF is a composition of carbon-bonded carbon fibers (CBCFs) that are layered to form a relatively dense, three-dimensional structure. The cylindrical sides of the GIS have a density of  $1.98 \text{ g/cm}^3$ . FWPF is extremely tough and has excellent thermal-shock resistance. The thermal conductivity and emissivity are anisotropic. The GIS is designed to absorb energy and cushion the fuel capsule under Earth impact conditions associated with GPHS module terminal velocity. The GIS also provides a protective shell against shrapnel that may penetrate the aeroshell and the CBCF sleeve.

## 2.4 Carbon-Bonded Carbon Fiber Disk and Sleeve

Surrounding each GIS is a thermal insulating sleeve constructed of CBCF-3. Developed by Oak Ridge National Laboratory, CBCF-3 has a density of only  $0.23 \text{ g/cm}^3$  and has a very low thermal conductivity normal to its deposition plane. At each end of the GIS is an insulating disk made of the same material. The primary function of the insulator is to prevent overheating of the fuel capsule during hypersonic reentry and overcooling during subsonic descent. It also provides protection against the heat from launch pad fires.



## **2.5 Aeroshell**

Four clad fuel pellets enclosed in two GISs and surrounded by the thermal insulators are housed in the outer aeroshell as shown in figure 1. Each of the two assemblies is held in place by an aeroshell cap and a lock screw. All aeroshell components are constructed of the same material as the GIS, FWPF graphite. The aeroshell is the primary structural member of the GPHS module. Its primary function is to provide ablation protection during reentry, thus protecting the GISs from the harsh environment encountered during reentry. It also serves as the outermost protective layer against shrapnel in the event of an explosion.

### 3. BACKGROUND

MSFC has established the capability to perform system level nonnuclear testing of radioisotope power systems. Electrically powered GPHS simulators have been developed that mimic the thermal and geometrical properties of the actual GPHS module at its boundaries (the external surface of the aeroshell). These individual GPHS simulators can be stacked in any configuration and integrated with a complete power conversion system including converter, control hardware, radiator, etc. The first versions of these simulators have been built and tested individually and as a three module 750 W thermal stack (fig. 2). This stack produces a total of 750 W of thermal power.

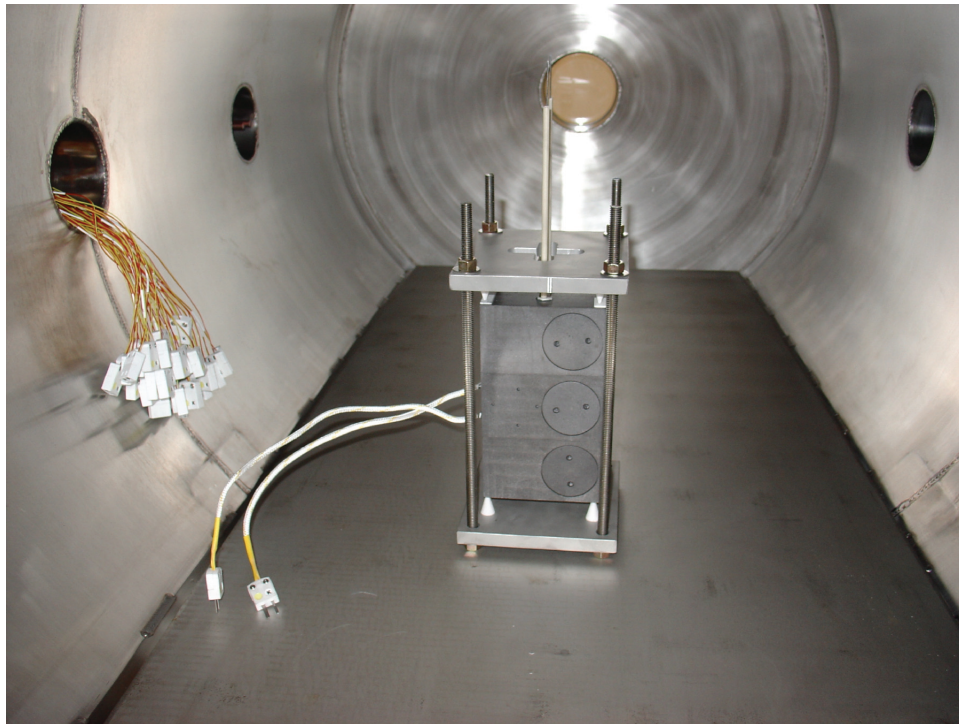


Figure 2. Three GPHS simulators stacked together inside a vacuum chamber at MSFC.

To effectively design and test an integrated system consisting of GPHS modules and a Stirling power converter, it is necessary to understand the coupled physics between the two. To begin this process, a conceptual trade study was performed for a total of six different GPHS stack configurations encompassing three different power levels.

### 3.1 Previous Work

Conceptual and detailed design studies of RPS have been performed for GPHS module powered Stirling converters in the past. Examples of some of the work that has been performed to date include: Glenn Research Center's (GRC) proposed "Next Generation Stirling Radioisotope Generator (SRG)" using a Sunpower, Inc. advanced Stirling converter.<sup>4</sup> This system could potentially provide 164 W at a specific power level of 8 W/kg (a significant improvement over existing thermoelectric systems in the 3 to 5 W/kg). Lockheed Martin Space Systems has performed detailed thermal analysis of individual GPHS modules with the boundaries radiating to a sink while also studying stack configurations containing 4, 8, and 12 modules.<sup>5</sup> Through a NASA grant, the University of Florida has performed a conceptual design for 250 W<sub>e</sub> and 500 W<sub>e</sub> configuration in which the GPHS modules were coupled to the Stirling converter by radiation.<sup>3</sup> With the exception of the work performed by GRC, operation at off-nominal conditions was not studied.

### 3.2 Description

The conceptual trade study was performed to understand how temperature varies between GPHS modules for a given stack geometry subject to both nominal and off-nominal conditions. The nominal case is defined as the design or normal operating condition while the off-nominal cases simulate a reduction in power demanded by the Stirling converter whether intentional or unintentional; e.g., a failure.

A typical configuration is illustrated in figure 3. This configuration produces 250 W of electrical power from 1,000 W of thermal power (four GPHS modules at 250 W each). The GPHS modules are coupled to the Stirling through a nickel plate and boot section (noted as the Stirling interface in fig. 3). The hot shoe of the Stirling converter is positioned within the nickel boot. Heat is conducted through the GPHS modules through the interface plate and boot and finally into the hot shoe of the Stirling. Sealed within the Stirling is a working fluid, that when heated, expands to drive a piston that in turn drives a converter (linear alternator) that produces electrical power. The Stirling converter cold shoe is used to remove waste heat from the system and is attached to a radiator. The higher the temperature difference between the hot and cold shoe, the higher the efficiency of the Stirling. Figure 4 shows an example efficiency curve for a 35 W<sub>e</sub> Stirling converter.<sup>6</sup> Hot and cold shoe temperatures cannot be set arbitrarily. The hot shoe temperature is limited by its material properties, while the cold shoe temperature is limited by the size of the radiator. The overall goal for the system is to achieve the highest specific power possible, where specific power is defined as generated electrical power divided by the mass of the overall power system (sum of all components). Radiator area scales as the inverse of its operating temperature is raised to the fourth power; therefore, a compromise must be made as to the cold shoe operating temperature. Typically, it is preferable to operate at as high a cold shoe temperature as feasible in order for the converter to keep radiator mass to a minimum.

$$A_{\text{radiator}} \propto \frac{\dot{Q}_{\text{radiator}}}{T_{\text{cold shoe}}^4} . \quad (1)$$

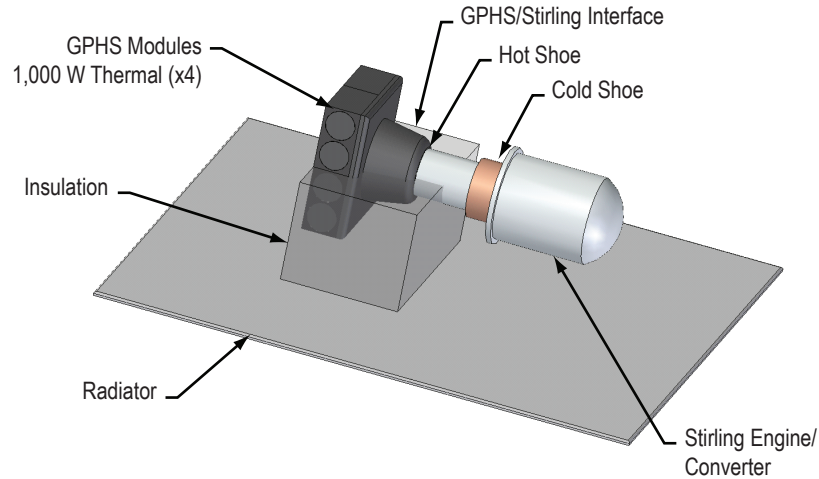


Figure 3. Example of a  $250 W_e$  stack configuration.

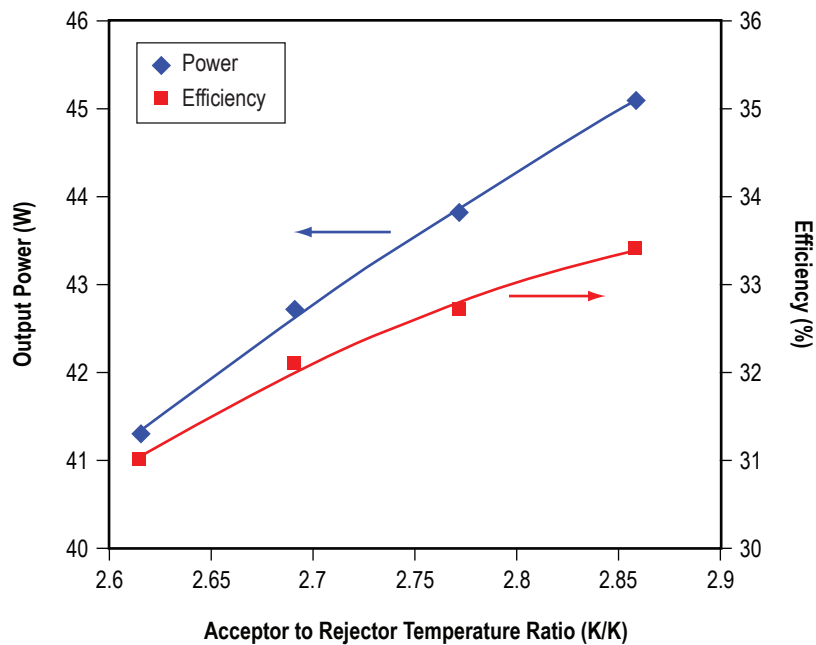


Figure 4. Example of an efficiency versus temperature ratio (hot shoe divided by cold shoe temperature) for a  $35 W_e$  Stirling converter.<sup>6</sup>

In order for the Stirling to operate at the desired power level, the appropriate amount of heat flux must be supplied to the hot shoe while maintaining the hot shoe at its predefined temperature. Both of these boundary conditions can be achieved by providing an appropriate amount of insulation around the GPHS modules and Stirling interface hardware. Assessing these parasitic losses is a key step to

evaluating the thermal power balance for a given configuration. The overall power balance is shown in equation (2):

$$W_{e\text{Stirling}} = \sum \dot{Q}_{\text{thermal}} - \sum \dot{Q}_{\text{radiation}} - \dot{Q}_{\text{radiator}} \quad (2)$$

Once an optimum configuration, from the standpoint of efficiency, has been established for a given nominal operating point, any reduction in power demanded by the Stirling converter will result in a temperature rise in all system components. The rate of temperature rise is dependent on a given stack configuration and its overall thermal efficiency at the nominal operating point. The higher the overall thermal efficiency, the more rapid the temperature rises, as less power is demanded by the Stirling. The temperatures and other performance parameters for each study configuration are described in appendix A.

### 3.3 Assumptions

Listed below are relevant assumptions that affect the thermal model used to calculate the required amount of multilayer insulation (MLI), GPHS module temperatures, and radiator size:

(1) Thermal energy is transferred through a GPHS module by its aeroshell only. The aeroshell is anisotropic with two values of thermal conductivity (73 W/m-K and 58 W/m-K).<sup>3</sup> These values are based on averaging data between 600 and 1,700 °C.

(2) Module to module and module to interface plate connections are joined by GRAFOIL<sup>®</sup> (developed by Graftech, Inc.), a material used to reduce the thermal contact resistance thereby improving heat transport.

(3) One-dimensional conduction is used in all three dimensions. However, where appropriate, a conduction shape factor is used to incorporate two-dimensional thermal effects (described in sec. 4.2).

(4) The GPHS modules and Stirling interface components radiate through MLI to a black body sink at 3 K. The emissivity of each GPHS module, interface plate component, and MLI sheet was assumed to be constant. The emissivity value (0.8) for the aeroshell was based on averaging data between 600 and 1,700 °C.<sup>3</sup> The emissivity of each sheet of MLI was assumed to be 0.1.

(5) The Stirling efficiency is held at a constant value of either 31 or 33 percent. These values are determined by selection of the hot and cold shoe nominal operating temperatures (sec. 3.2).

(6) The radiator operating temperature is held equal to the Stirling converter's cold shoe temperature, and it radiates to a black body sink at 3 K.

### 3.4 Modeling Tools

The following briefly describes the two software packages used to perform the work described within this TM studies of interest:

(1) MATLAB<sup>®</sup> (marketed by The Mathworks, Inc.) was used in order to rapidly develop and debug the methodology used to solve for temperature profiles within a given GPHS stack configuration, to determine the required amount of MLI, to analyze off-nominal operating points, and to perform radiator sizing. MATLAB is a programming language as well as a command-line interpreter. It contains a vast amount of mathematical and data visualization functions. Program data can be accessed in debug mode and modified at run time through the command line.

(2) Patran<sup>®</sup> (marketed by MSC Software), a two- and three-dimensional stress and thermal analysis tool, was used to calculate the two-dimensional conduction shape factor for the GPHS module (sec. 4.2). Patran was selected because of its availability, familiarity of operation, and the need for a quick turn-around time.

#### 4. APPROACH

A total of six design configurations were evaluated encompassing three different power levels. Only a representation of the GPHS modules, interface hardware, and insulation are shown in figure 5.

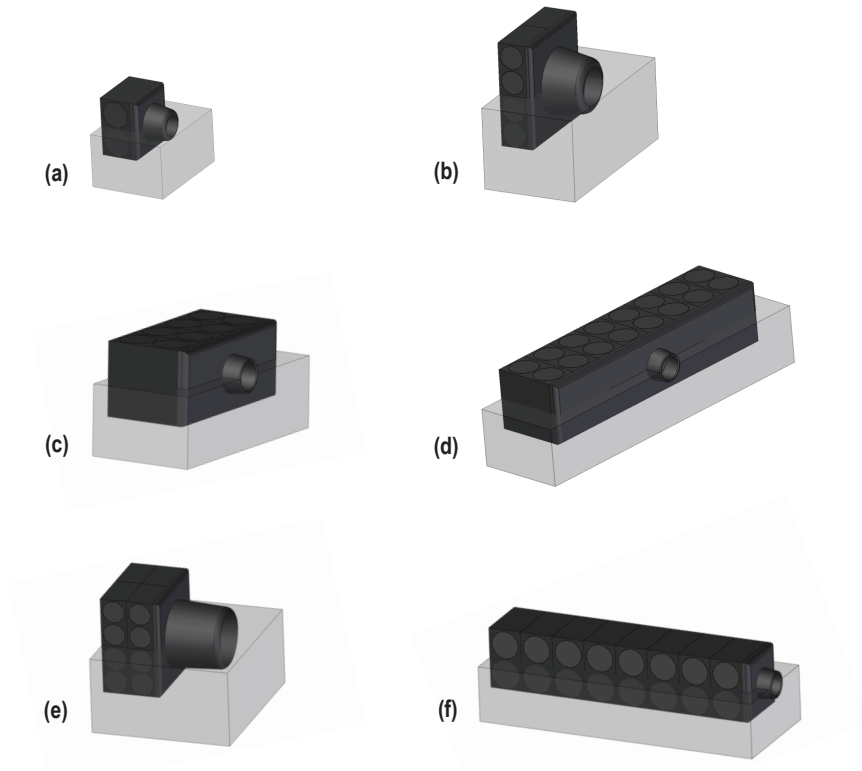


Figure 5. The six stack configurations analyzed in the trade study: (a)  $80 W_e$ , (b)  $250 W_e$  configuration 1, (c)  $250 W_e$  configuration 2, (d)  $500 W_e$  configuration 1, (e)  $500 W_e$  configuration 2, and (f)  $500 W_e$  configuration 3.

These cases were selected because thermal power is transported from the GPHS modules to a Stirling interface plate by conduction through the modules themselves and not by wrapping module stacks in highly conductive material or using some means of active heat transport; e.g., heat pipes. For this reason these geometries are deemed “worst case” scenarios when considering the potential for exceeding GPHS module temperature limits. It should be noted that it was assumed that a highly conductive material (GRAFOIL) was inserted between the individual modules in order to reduce thermal contact resistance.

## 4.1 Radiator Sizing

Although the Stirling converter would be highly efficient, it is still a heat engine and limited by the Carnot cycle efficiency; therefore excess energy must be removed. This would be accomplished using a radiator for space applications. In order to size the radiator, its operating environment must be established. For this conceptual study, it was assumed that the radiator radiated to a space environment of 3 K and has an emissivity of 0.9 W/(m<sup>2</sup>-K). It was also assumed that the radiator operated at the cold side temperature of the Stirling (assuming heat pipes are employed). Given this information, the following relationship can be used to determine the amount of heat energy the radiator must dissipate:

$$\dot{Q}_{\text{radiator}} = (1 - \eta_{\text{Stirling}}) \dot{Q}_{\text{Stirling}} = \left( \frac{1 - \eta_{\text{Stirling}}}{\eta_{\text{Stirling}}} \right) W_e . \quad (3)$$

Once the magnitude of waste heat is established, the radiator area can be determined:

$$A_{\text{radiator}} = \frac{\dot{Q}_{\text{radiator}}}{\sigma \epsilon (T_{\text{radiator}}^4 - T_{\text{space}}^4)} . \quad (4)$$

## 4.2 Nominal Analysis

Figure 6 depicts a flow chart representation of the steps involved in performing the nominal and the off-nominal analysis.

To judge the validity of a given configuration, the temperature distribution across the GPHS module stack is calculated. This is accomplished by evaluating a steady state power balance for each configuration assuming one-dimensional conduction in all three dimensions between GPHS modules and across the interface plate. Each GPHS module is treated as a single mass entity at an average temperature while the interface plate is divided into multiple mass elements corresponding to each GPHS module in contact with it. The entire configuration is insulated except for the area of the interface plate that is in contact with the Stirling converter hot shoe. At this contact point, the thermal energy drawn by the Stirling unit is assumed to be distributed evenly over each of the interface plate sections that come in direct contact with it.



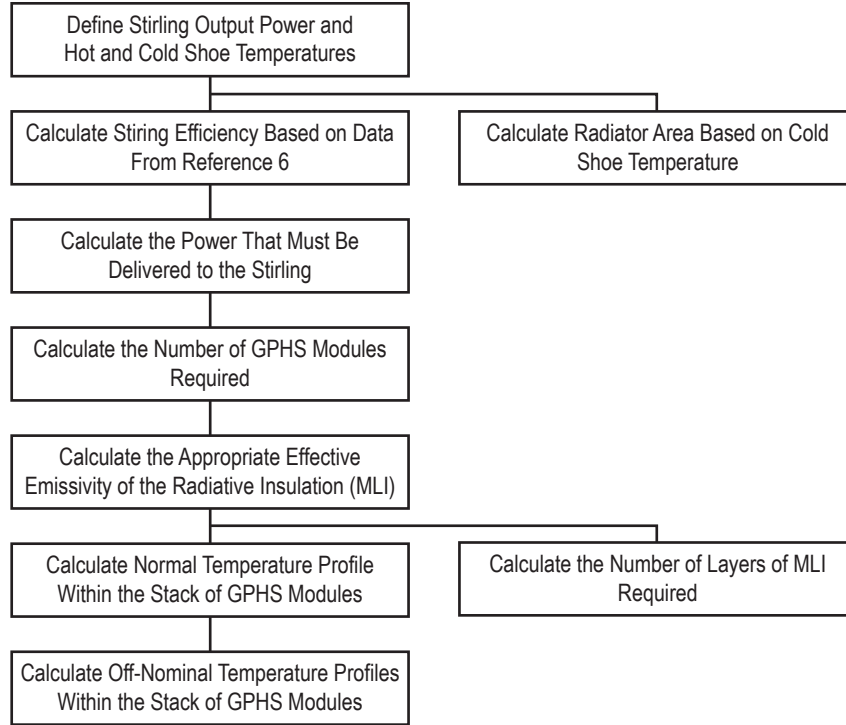


Figure 6. Flow chart representation of the steps taken to obtain the results presented in this study.

The total resistance to heat flow through all of the components in the CBCF sleeve is much greater than through the block structure of the aeroshell. For this reason it was assumed that thermal power was conducted from module to module through the aeroshell alone. Because one-dimensional heat conduction is used to determine the power balance, a conduction shape factor was generated in order to capture two-dimensional conduction phenomena, improving predictive capability of the analysis (fig. 7). The shape factor was generated by analyzing a two-dimensional thermal model of the aeroshell in Patran, and by determining the heat flux through the aeroshell with the boundary conditions given in figure 7. The shape factor can then be calculated as follows:

$$S_{\text{conduction}} = \frac{\dot{Q}}{\Delta T} = \frac{kA}{\Delta x} . \quad (5)$$

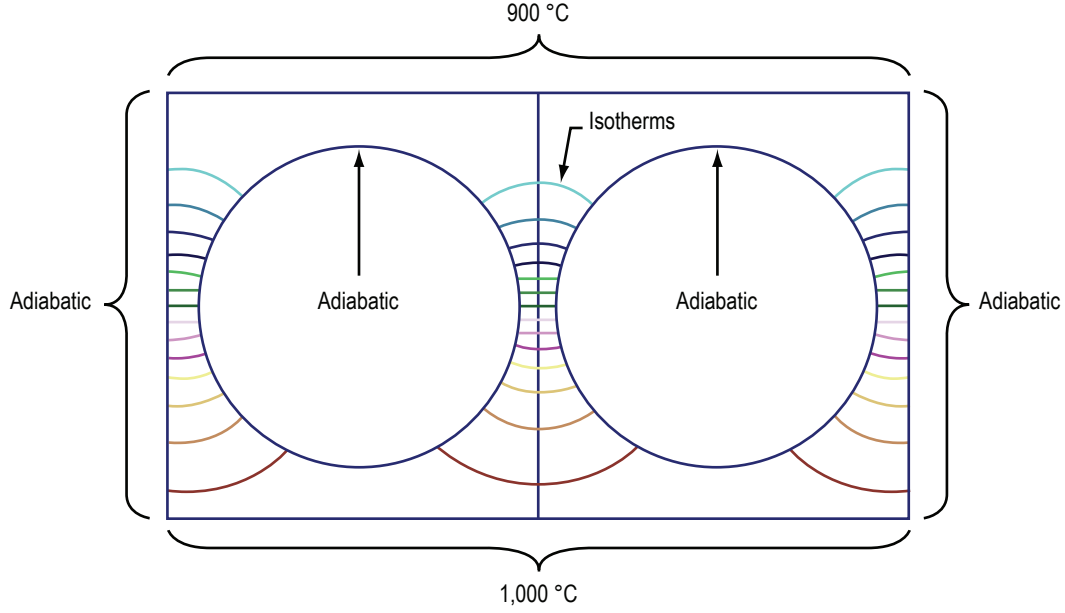


Figure 7. Two-dimensional model of heat conduction through aeroshell used to determine the conduction shape factor.

The shape factor is applied only along the vertical axis shown in figure 7. Because of the symmetry of the chosen stack configurations, it was assumed that no heat was conducted between modules along the horizontal axis. This same approach was applied to the axis perpendicular to the page where heat conduction was assumed to be one-dimensional so no shape factor was applied. Radiative heat transfer (environmental losses) was assumed around the entire boundary of the stack and interface plate except where directly connected to the Stirling. The boundary condition at the Stirling was dictated by the power demands of the Stirling.

In order to perform the analysis for a given configuration, the Stirling output power, hot side temperature, and cold side temperature were selected. Based on the hot and cold side temperatures, the Stirling converter efficiency could be determined using the data from reference 6 (fig. 4). The power supplied to the Stirling from the GPHS modules can be calculated as follows:

$$\dot{Q}_{\text{Stirling}} = \frac{\dot{W}_{\text{eStirling}}}{\eta_{\text{Stirling}}} . \quad (6)$$

Now the number of GPHS modules required to supply the Stirling can be determined (each module supplies 250 W of thermal power). Margin must be included to account for heat loss to the environment; for this study, the loss is assumed to be purely radiative. To maximize the power available to the Stirling from the GPHS modules, the stack must be insulated so that thermal losses are minimized:

$$\dot{Q}_{\text{thermal}} - \dot{Q}_{\text{radiation}} = \dot{Q}_{\text{Stirling}} = \frac{\dot{W}_{\text{eStirling}}}{\eta_{\text{Stirling}}} . \quad (7)$$

The next step is to determine the required number of layers of MLI necessary to meet this goal. It is assumed that each layer of MLI is at a constant temperature. Equation (8) is used to represent the heat flow from a GPHS module surface through the MLI:

$$\dot{Q} = \frac{A\sigma(T_{\text{gphs}}^4 - T_{\text{inf}}^4)}{\frac{1 - \epsilon_{\text{gphs}}}{\epsilon_{\text{gphs}}} + \frac{1}{F_{\text{gphs}}} + (n-1) \left( \frac{1 - \epsilon_s}{\epsilon_s} + 1 \right)}, \quad (8)$$

where  $n$  is the number of layers of insulation to be used. Rather than solving for the integer value of  $n$  that meets the power requirements of the Stirling, an effective emissivity is defined and used to back out the number of layers of MLI required. Equation (8) can now be rewritten in terms of the effective emissivity and expressed as:

$$\dot{Q} = A\sigma\epsilon_{\text{effective}}(T_{\text{gphs}}^4 - T_{\text{inf}}^4). \quad (9)$$

The effective emissivity is defined as the following:

$$\epsilon_{\text{effective}} = \frac{1}{\frac{1 - \epsilon_{\text{gphs}}}{\epsilon_{\text{gphs}}} + \frac{1}{F_{\text{gphs}}} + (n-1) \left( \frac{1 - \epsilon_s}{\epsilon_s} + 1 \right)}. \quad (10)$$

Once the effective emissivity is determined, the number of layers ( $n$ ) of MLI can be determined:

$$n = \frac{\frac{1}{\epsilon_{\text{effective}}} - \left( \frac{1 - \epsilon_{\text{gphs}}}{\epsilon_{\text{gphs}}} + \frac{1}{F_{\text{gphs}}} \right)}{\frac{1 - \epsilon_s}{\epsilon_s} + 1} + 1. \quad (11)$$

The problem is still to resolve the appropriate effective emissivity. This is accomplished by assessing the power balance for many different values of the effective emissivity given the appropriate heat flux boundary condition to the Stirling converter. This results in a plot of Stirling interface temperature versus the effective emissivity<sup>7</sup> of the MLI. Figure 8 provides an example for a 250 W<sub>e</sub> configuration.

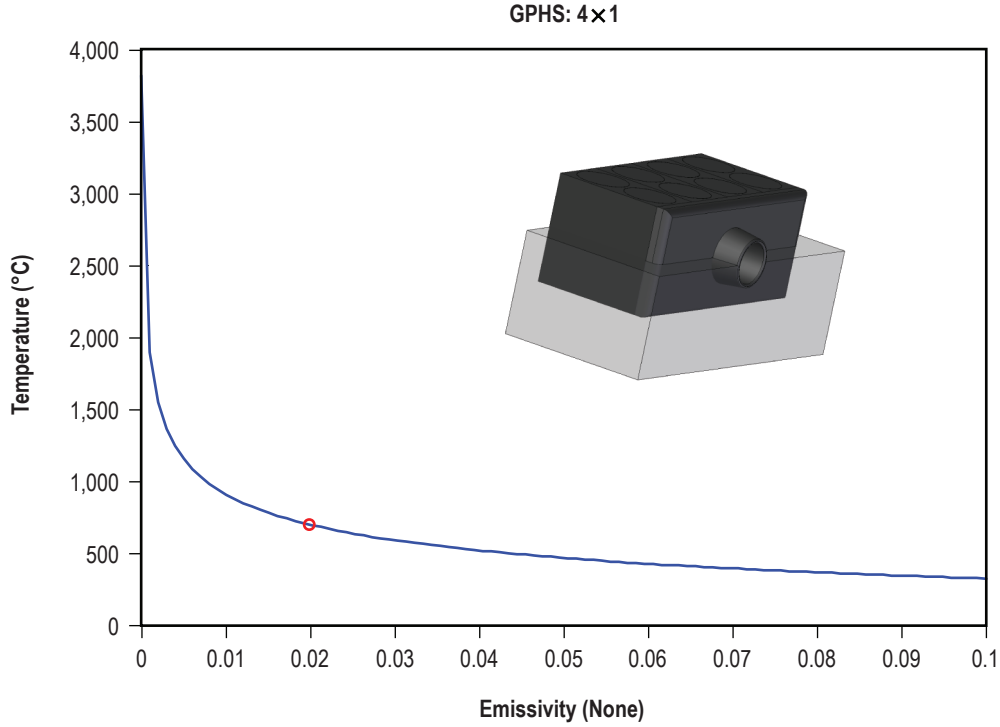


Figure 8. Example of Stirling interface temperature as a function of the effective emissivity.

The value of the effective emissivity that will achieve an interface temperature of 700 °C is found by interpolating the data used to generate figure 8, and in this example, is indicated by a circle on the temperature graph. This condition provides a temperature gradient of 50 °C between the Stirling interface and hot shoe in order to ensure that a 650 °C hot shoe temperature can be maintained (at nominal rated power).

At this point, sufficient information is available to calculate the temperature profile throughout the GPHS stack. This is accomplished by applying a power balance to each component in the system. For each GPHS module,

$$\dot{Q}_{\text{generated}} + \sum_{\text{in}} \dot{Q}_{\text{conducted}} = \sum_{\text{out}} \dot{Q}_{\text{conducted}} + \sum_{\text{out}} \dot{Q}_{\text{radiated}} \quad (12)$$

For each interface plate section,

$$\sum_{\text{in}} \dot{Q}_{\text{conducted}} = \sum_{\text{out}} \dot{Q}_{\text{conducted}} + \sum_{\text{out}} \dot{Q}_{\text{radiated}} + \sum_{\text{out}} \dot{Q}_{\text{Stirling}} \quad (13)$$

The relationships written for each GPHS module and each interface plate section result in a coupled system of linear and nonlinear equations in which the temperatures in each component can be solved. The Gauss Seidel iteration method was used to obtain the solution. This method was chosen because it is efficient from both a programming time and memory standpoint for solving equations that can be readily linearized and expressed in an explicit format. An explicit format implies that each equation is written to explicitly calculate the value of the unknown for that equation, in this case, temperature. However, in order to perform this operation, the nonlinear radiation terms must be linearized:

$$\dot{Q}_{\text{radiation}} = \sigma A \epsilon (T_1^4 - T_2^4) = \sigma A \epsilon \left( (T_1^2 + T_2^2)(T_1 + T_2) \right)_{i-1} (T - T_2) . \quad (14)$$

The terms in parenthesis subscripted by  $i-1$  are evaluated based on the temperatures at the previous iteration. After a reasonable initial guess for the temperature distribution is supplied to the model, the iteration proceeds and terminates only when the calculated power into each component is equal to the calculated power leaving each component within some specified tolerance. The results for a  $250 W_e$  configuration are illustrated in figure 9. The graphical data show temperature curves for the hottest GPHS module and Stirling interface plate as a function of power demanded by the Stirling. For this case, the normal operating temperatures are given when the Stirling is operating at  $250 W_e$ . As the power demanded by the Stirling is reduced, temperatures increase (as expected); however, even at complete Stirling failure, the maximum GPHS module temperature remains below the  $1,300^\circ\text{C}$  limit. The table to the right in figure 9 provides information regarding boundary conditions and performance at the nominal operation point.

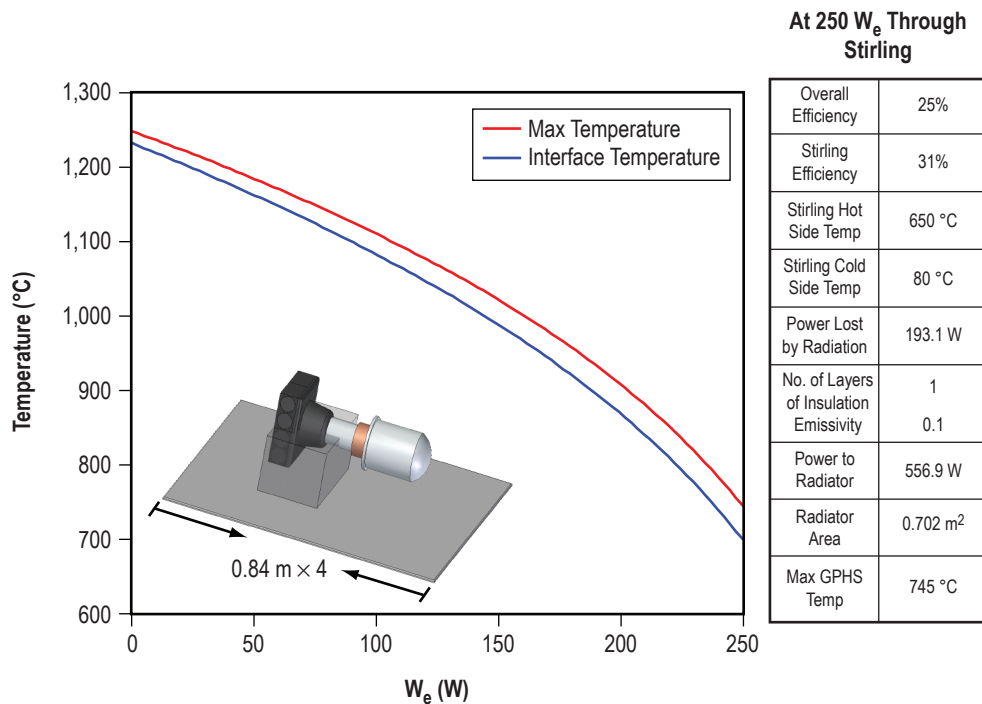


Figure 9. Analysis results for the  $250 W_e$  configuration 1. (Stirling efficiencies are from data provided in reference 6.)

### 4.3 Off-Nominal Analysis

Once the initial nominal power balance was completed, off-nominal cases were examined. This was accomplished by varying the boundary condition that specifies power demanded by the Stirling; for the study, this consisted of small steps ranging from nominal to zero power. At each increment, the temperature solutions are recalculated so that a plot of temperature versus power demanded is generated. As power demand drops off, the temperatures throughout the configuration increase. The heat flux that was being provided to the Stirling now must be dissipated through the MLI that has a high resistance to heat flow. This high resistance dictates a higher internal temperature in order to remove the excess power. How fast the temperature increases relative to the difference in power demanded between the nominal and off-nominal points is a function of the overall system efficiency at nominal operating conditions. As the ratio of power lost due to radiation to the thermal power delivered by the stack of GPHS modules decreases (a thermally more efficient stack), the rate at which the temperature increases for off-nominal points increases. The results of all six study cases are provided in appendix A. For the six cases traded, the 80  $W_e$  power level must operate at the highest efficiency; therefore, it is expected to have the most rapid increase in stack temperatures at off-nominal points. The off-nominal results for a 250  $W_e$  case are shown in figure 8. The curves indicate the average temperature in the hottest GPHS module for the given configuration as well as the interface temperature as a function of power demanded by the Stirling. Therefore, the plot represents the results for both the nominal and off-nominal cases.

## 5. FUTURE WORK

Potential follow-on activities should be directed toward investigating more conducive methods of passing heat from the GPHS modules to the Stirling hot shoe. One option would be to use a highly conductive shunt (such as K-Core™, marketed by K Technology Corporation) positioned around and/or between the GPHS modules to remove the heat from the GPHS modules and deliver it more efficiently to the Stirling hot shoe. Another option would be to use an active means of heat transport, such as heat pipes, that would wick the heat from the GPHS modules to the Stirling. These options would allow for lower overall operating temperatures within the GPHS modules while also providing some margin for off-nominal operation.

Another topic of interest involves addressing a method or technique for removing excess energy from the system and dumping it to the environment in the event of off-nominal operation. This can be accomplished by using active heat pipes (ref. 4) or by providing a variable conduction coupling path to a radiator. The conduction technique could be a passive means that would be initiated by the thermal expansion of components closing a very thin radiation gap producing a highly conductive path to a radiator. This gap would be closed only in the event of elevated temperatures caused by off-nominal operation.

As specific designs that incorporate enhanced heat transfer attributes begin to mature, a more detailed thermal analysis coupled with nonnuclear testing should be performed. This approach will either disprove or provide confidence in the design as well as identify integration issues not identified by mathematical analysis of the system.

## 6. SUMMARY

To effectively design and test an integrated GPHS module and Stirling converter power system, it is necessary to understand the coupled physics between the components. A conceptual trade study was used to start this process by examining six different GPHS stack configurations at a total of three different power levels (80, 250, and 500  $W_e$ ). The trade was performed to understand temperature variation between GPHS modules for given stack geometries subject to both nominal and off-nominal conditions. The nominal case consists of normal design operating conditions while the off-nominal cases simulate a reduction in power demanded by the Stirling converter whether intentional or unintentional; e.g., a failure. The calculated temperatures are average temperatures and a more refined analysis must be performed in order to increase the fidelity of these results which are as follows:

(1) It is important that the overall system be as efficient as possible (in a thermal sense) in order to achieve a high level of specific power. However, the more efficient the system, the more rapid the temperature increase within the stack for off-nominal power conditions. This could result in more complicated methods of achieving active heat rejection in the case of Stirling failure that, in turn, results in a lower specific power. In order to achieve the highest specific power number that provides confidence in creating a working system, a balance must be made between efficiency and heat rejection capabilities.

(2) Only the “250  $W_e$  Configuration 1” (sec. A.2) and the “500  $W_e$  Configuration 1” (sec. A.4) have the ability to operate at significantly degraded output power levels while not exceeding the GPHS module temperature requirements of 1,300 °C. This is due both to the way in which the GPHS modules are stacked and to the fact that they are not highly efficient configurations.

(3) It is important to minimize radiator area and, therefore, radiator weight, but not necessarily at the expense of running at an increased cold shoe temperature that would reduce the overall Stirling efficiency. This reduction in Stirling efficiency would result in an increase in the number of GPHS modules in the system, thereby increasing system mass and reducing the system specific power.

(4) A method to remove excess power from the system at off-nominal operating conditions must be included in the design due to the following:

- An internal GPHS module temperature increase is expected to occur based on a more refined thermal analysis.
- Both configurations mentioned in (2) are marginally acceptable at low output power levels.

Each parameter in the system is coupled, and changing one affects all others (Stirling efficiency, hot shoe temperature, cold shoe temperature, radiator size, number of GPHS modules, overall efficiency, and specific power). The optimum system configuration will be one that maximizes the value of specific power by trading off system complexities and packaging requirements. The best approach for the cases examined occurred when the heat was transported through the stack of GPHS modules along the most conductive axis of the aeroshell—the aeroshell is anisotropic—to the interface plate by means of the shortest distance possible.



## APPENDIX A—RESULTS FOR ALL STUDY CASES

Results for six study configurations at a total of three different power levels are presented in this appendix. A summary of the results is presented in table 1. The “Stack Configuration” row designates the number of GPHS modules used and the way in which they were stacked for a given configuration. The “Power Check” row is the total power input by the GPHS modules minus the sum of the losses from the insulation and the radiator, corresponding to the electrical power generated by the Stirling converter. The “Hot Temp” and “Cold Temp” rows are the Stirling hot and cold shoe temperatures, respectively. The “Max Temp” row is the maximum temperature of the GPHS modules for the nominal point. All other rows are self-explanatory.

Table 1. Summary of results for all pertinent parameters for the six cases that were considered.

Electrical Power (W)	80	250		500		
Stack configuration	1×1	2×2	4×1	2×2×2	1×8	8×1
Power check	80	250	250	500	500	500
Efficiency (none)	0.326	0.309	0.309	0.309	0.309	0.309
Hot temp (°C)	700	650	650	650	650	650
Cold temp (°C)	80	80	80	80	80	80
$\dot{Q}_{\text{thermal}}$ (W)	250	1,000	1,000	2,000	2,000	2,000
$\dot{Q}_{\text{radiation}}$ (W)	4.54	193.07	193.07	386.14	386.14	386.14
$\dot{Q}_{\text{Stirling}}$ (W)	245.46	806.93	806.93	1,613.86	1,613.86	1,613.86
$\dot{Q}_{\text{radiator}}$ (W)	165.46	556.93	556.93	1,113.86	1,113.86	1,113.86
Radiator temp (°C)	80	80	80	80	80	80
Radiator area (m <sup>2</sup> )	0.1673	0.702	0.702	1.403	1.403	1.403
Max temp (°C)	751.7	745.3	880.3	851.4	2,688.4	1,256.5

### A.1 Study Case for 80 W<sub>e</sub> Configuration

This configuration operates at the highest overall efficiency (32 percent) of any of the six study cases. In order to meet the 80 W<sub>e</sub> power level with one GPHS module, the Stirling must operate at an efficiency of 32.6 percent. In order to achieve this efficiency, the Stirling hot shoe temperature was raised above the nominal choice of 650 to 700 °C. It should also be noted that only 4 W of power are lost to the environment via radiation, a highly improbable condition in reality when taking into account mounting, etc. Because this case operates at a higher efficiency than the others, it also has the most rapid temperature increase at off-nominal power levels. If two GPHS modules are used, the efficiency and specific power are more representative of the other configurations. Other system parameters of interest are shown in the table included with figure 10.

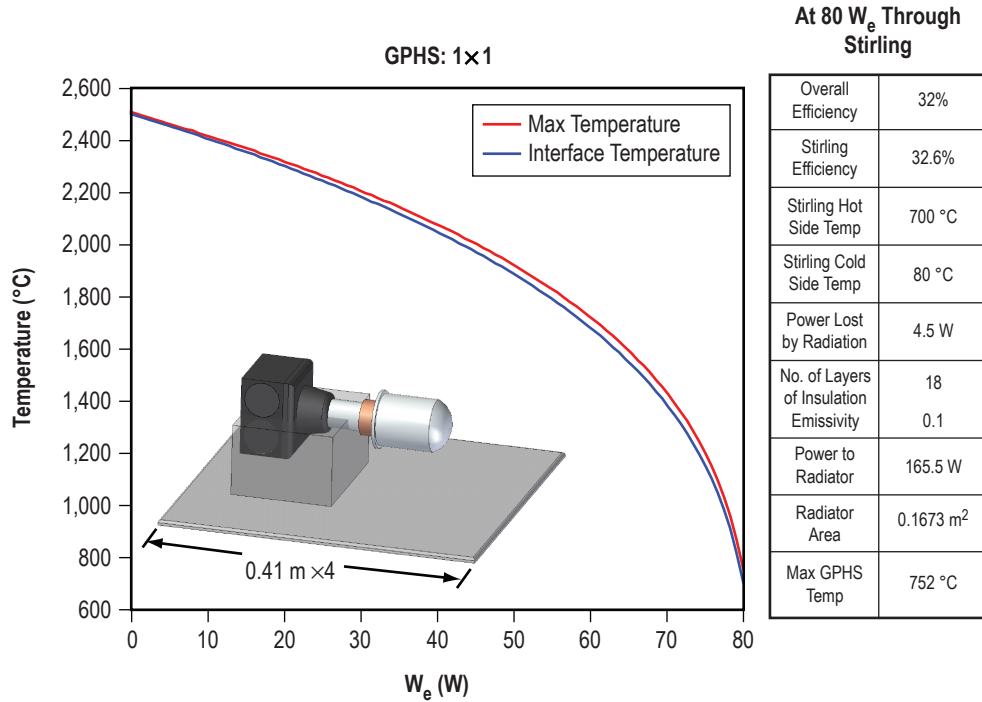


Figure 10. Analysis results for the 80  $W_e$  configuration. (Stirling efficiencies are from data provided in reference 6.)

### A.2 Study Case for 250 $W_e$ Configuration 1

This configuration operates at an overall efficiency of 25 percent and a Stirling efficiency of 31 percent. The hot shoe temperature is 650 °C in contrast to the 80  $W_e$  700 °C. The power lost to the environment by radiation is a more reasonable 193 W, implying that this configuration is much more realistic than the 80  $W_e$ . Other system parameters of interest are listed in figure 11.

### A.3 Study Case for 250 $W_e$ Configuration 2

This configuration operates at the same efficiencies and hot and cold shoe temperatures as the previous 250  $W_e$  configuration (25 percent, 650 °C, 80 °C). Its power lost to the environment due to radiation is also the same (193 W), however it has a different value of effective emissivity (fig. 12) and a different temperature profile (fig. 13). It must operate at higher temperatures than the 250  $W_e$  configuration 1 condition due to the stack arrangement of the GPHS modules. The configuration 2 arrangement is less effective at transferring power to the Stirling. (It has a higher overall thermal resistance.)

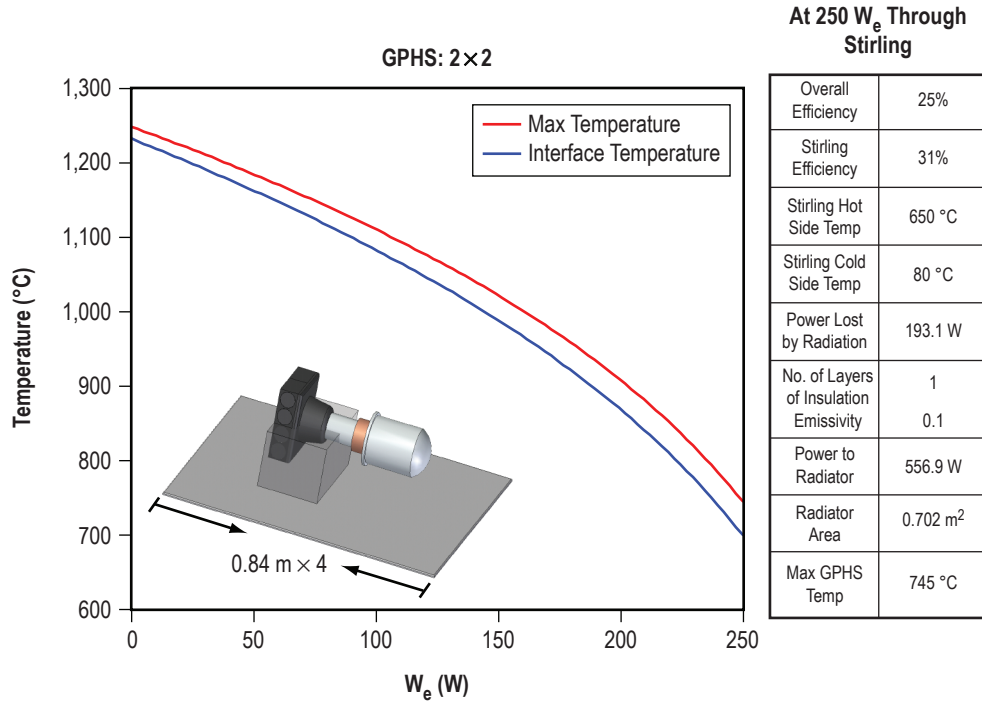


Figure 11. Analysis results for the 250  $W_e$  configuration 1. (Stirling efficiencies are from data provided in reference 6.)

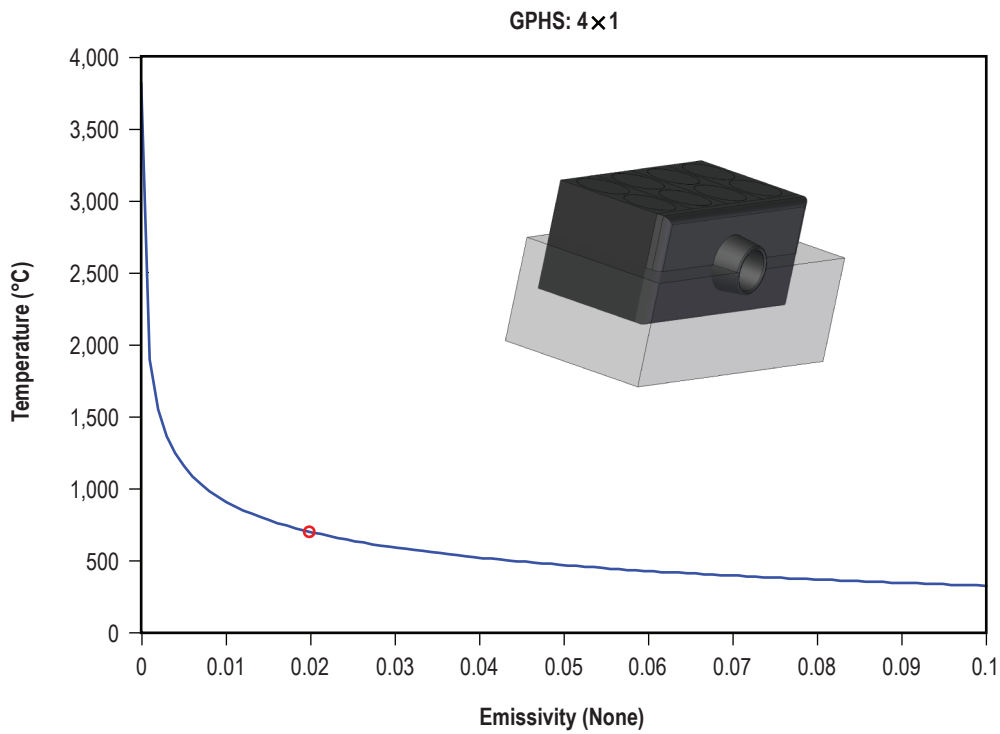


Figure 12. Stirling interface temperature as a function of effective emissivity for the 250  $W_e$  configuration 2.

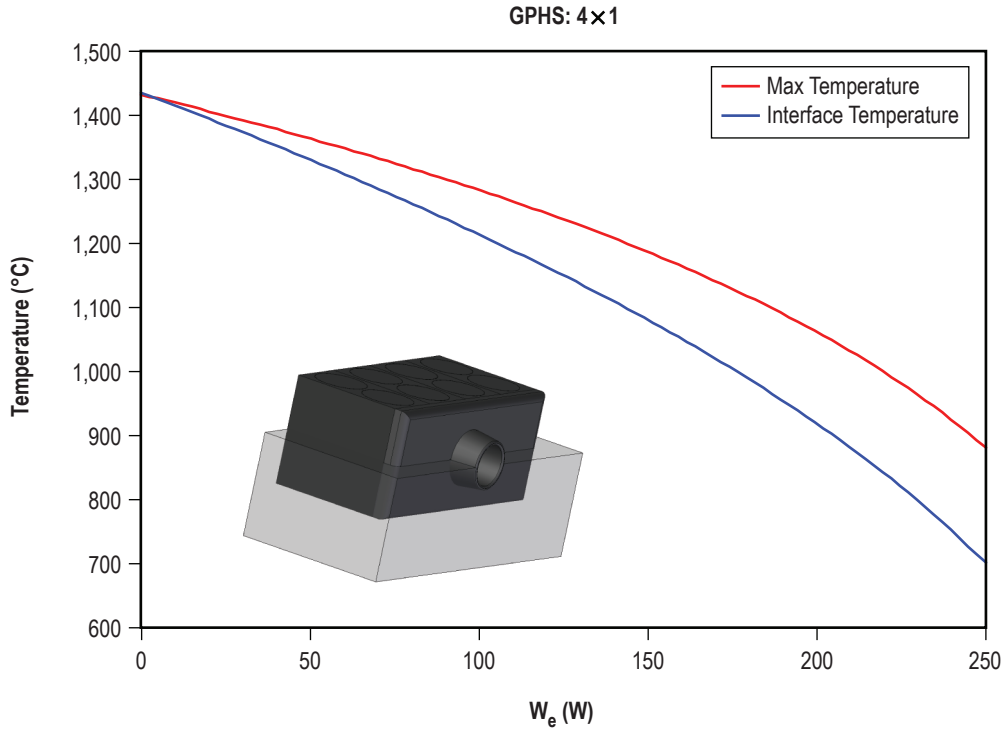


Figure 13. Maximum GPHS module temperature and interface temperature as a function of power demanded by the Stirling for the 250  $W_e$  configuration 2.

#### A.4 Study Case for 500 $W_e$ Configuration 1

This configuration operates at an overall efficiency of 25 percent and a Stirling efficiency of 31 percent. The hot shoe temperature is 650 °C, while the cold shoe temperature is 80 °C. The power lost to the environment by radiation is 386.14 W. Other system parameters of interest are shown in the table included in figure 14.

#### A.5 Study Case for 500 $W_e$ Configuration 2

This configuration operates at the same efficiencies and hot and cold shoe temperatures as the previous 500  $W_e$  configuration (25 percent, 650 °C, 80 °C). Its power lost to the environment by radiation is also the same (386 W). However, it has a different value of effective emissivity (fig. 15) and a different temperature profile (fig. 16). It must operate at higher temperatures than the 500  $W_e$  configuration 1 due to the arrangement of the stack of GPHS modules. This configuration has significant thermal resistance (due to the end-to-end stacking arrangement) and exceeds the maximum GPHS module temperature (1,300 °C) at the nominal operating point.

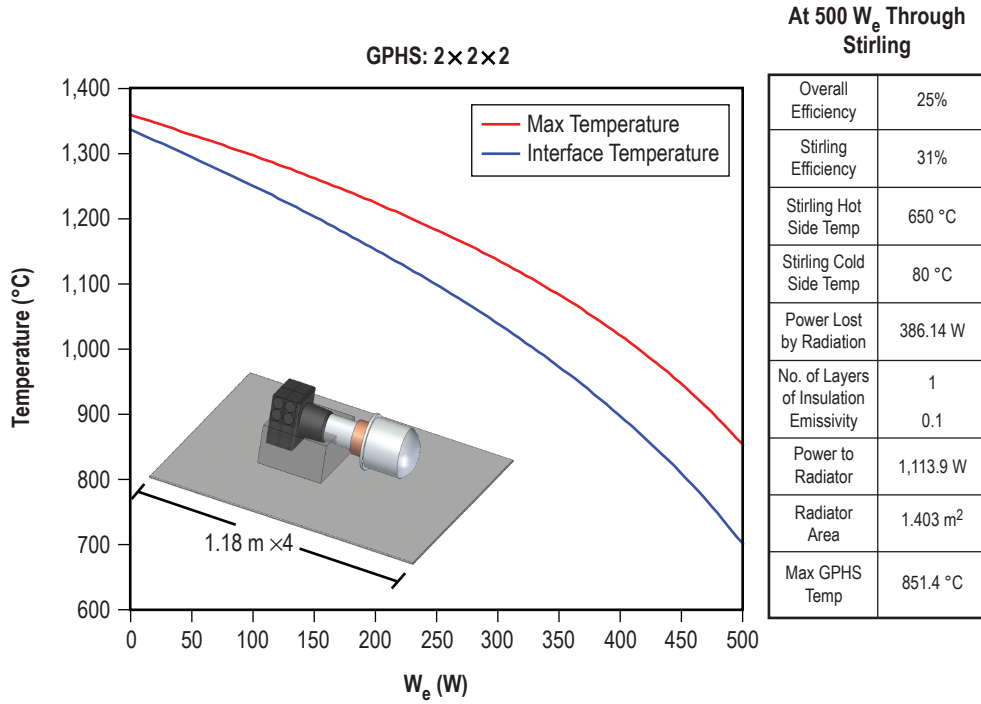


Figure 14. Analysis results for the 500  $W_e$  configuration 1. (Stirling efficiencies are from data provided in reference 6.)

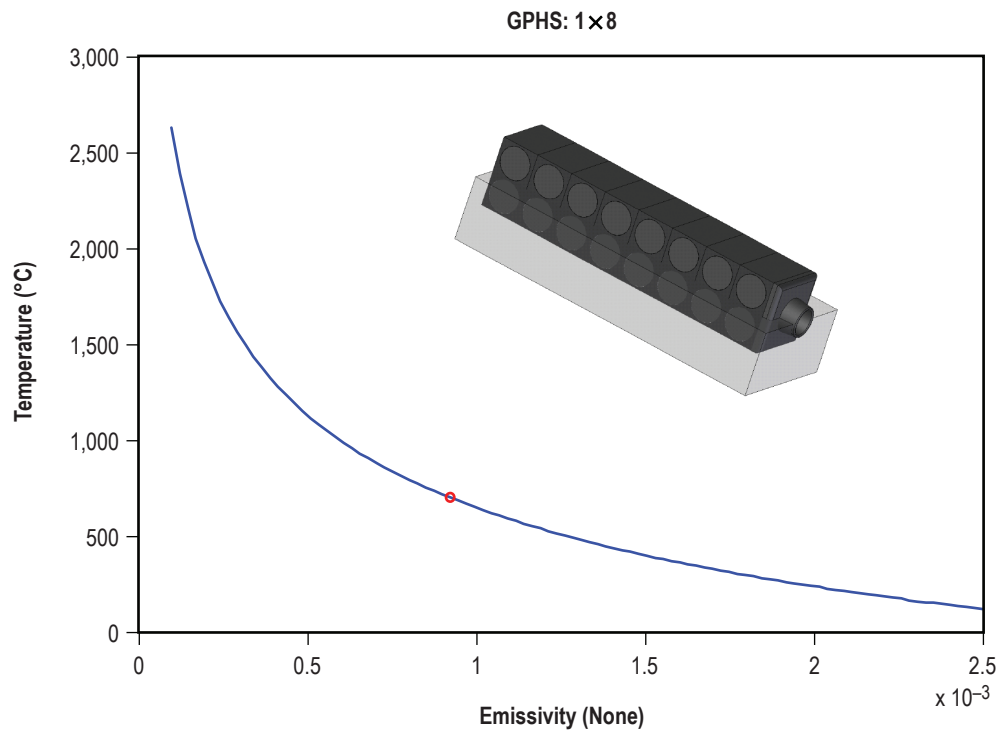


Figure 15. Stirling interface temperature as a function of effective emissivity for the 500  $W_e$  configuration 2.

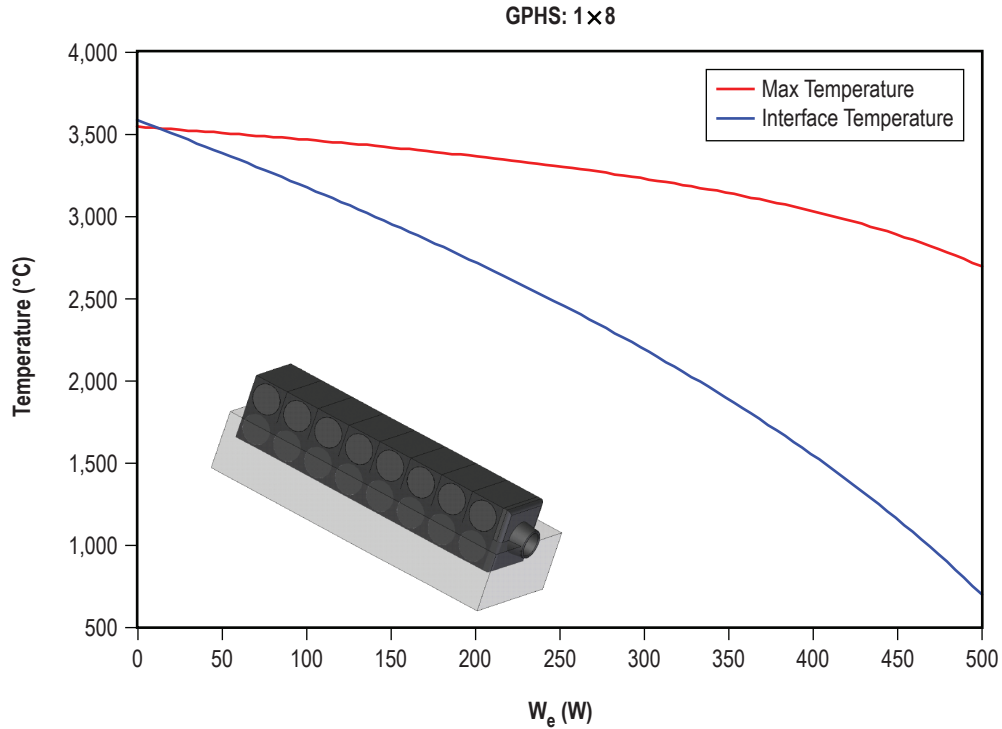


Figure 16. Maximum GPHS module temperature and interface temperature as a function of power demanded by the Stirling for the 500  $W_e$  configuration 2.

### A.6 Study Case for 500 $W_e$ Configuration 3

This configuration operates at the same efficiencies and hot and cold shoe temperatures as the previous 500  $W_e$  configurations (25 percent, 650 °C, 80 °C). Its power lost to the environment due to radiation is also the same (386 W). However, it has a different value of effective emissivity (fig. 17) and a different temperature profile (fig. 18). It must operate at higher temperatures than configuration 1 due to the arrangement of the stack of GPHS modules. This configuration is less effective at transferring power to the Stirling and, as such, is operating just below the maximum GPHS module temperature (1,300 °C) at the nominal design point.

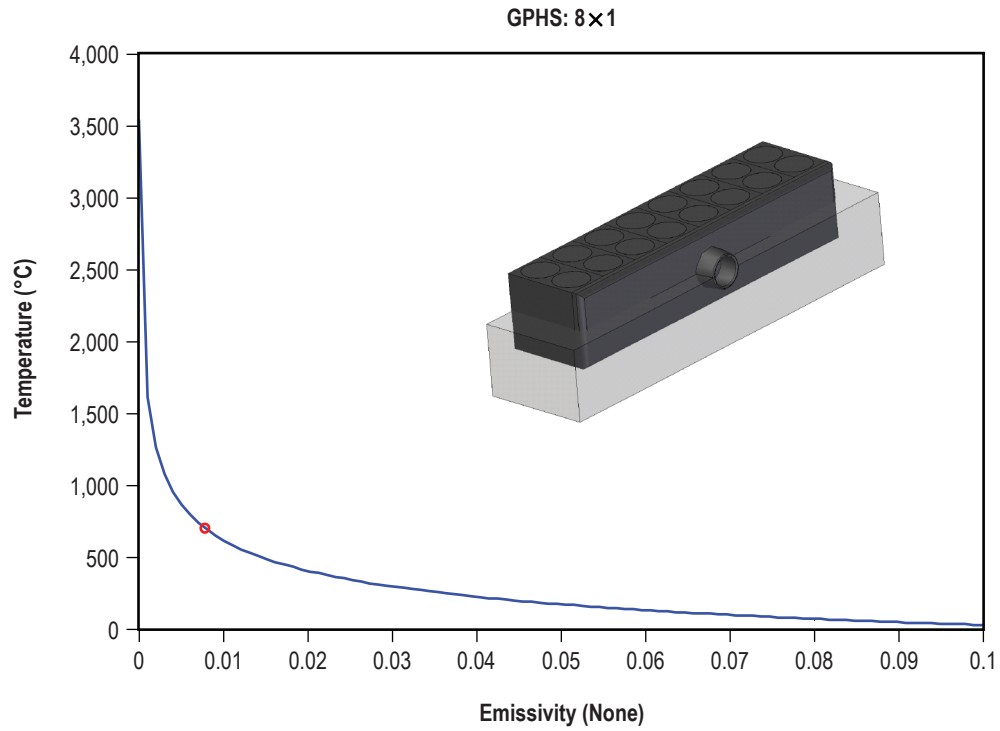


Figure 17. Stirling interface temperature as a function of effective emissivity for the 500  $W_e$  configuration 3.

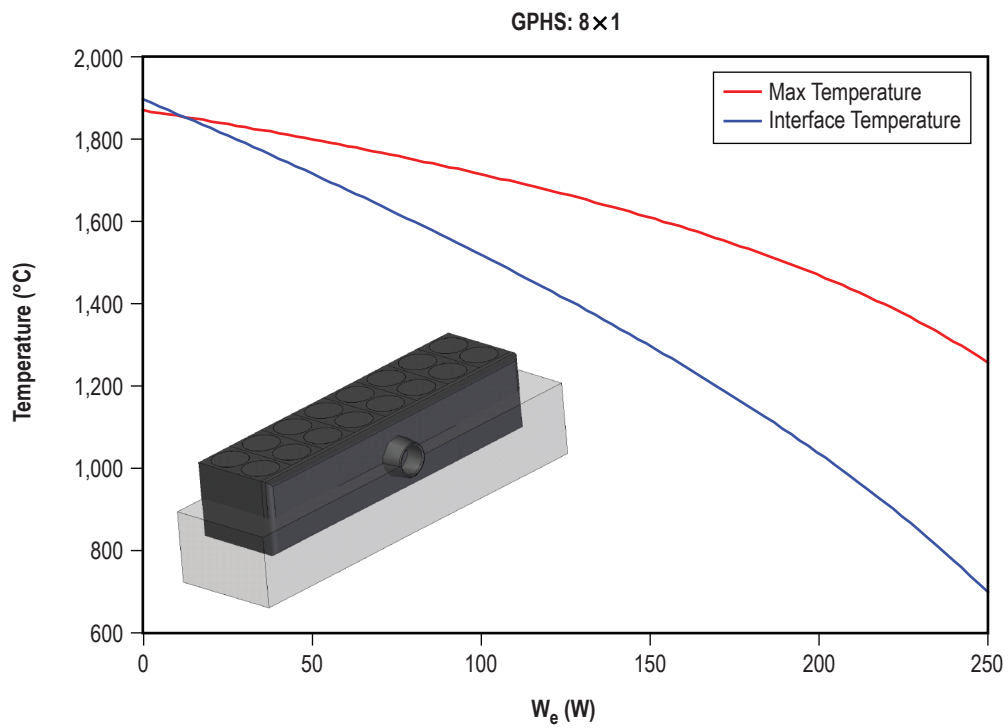


Figure 18. Maximum GPHS module temperature and interface temperature as a function of power demanded by the Stirling for the 500  $W_e$  configuration 3.





## REFERENCES

1. Van Dyke, M.; Houts, M.; Godfroy, T.; Dickens, R.; et al.: “Test Facilities in Support of High Power Electric Propulsion System,” *Proceedings of the Space Technology and Applications International Forum* (STAIF 2003), Albuquerque, NM, February 2–5, 2003.
2. Wagner, D.; Van Dyke, M.; Martin, J.; and Fazah, M.: “MSFC Advanced Skutterudite Thermoelectric Converter Development Proposal Inputs,” NASA /Marshall Space Flight Center Internal Document, *ER11-05-GPHS-001*, October 11, 2005.
3. McComas, T.J.; and Dugan, E.T.: “Thermal Analysis of Conceptual Designs for GPHS/FPSE Power Systems of 250 W<sub>e</sub> and 500 W<sub>e</sub>,” NASA—CR—187145, NASA Lewis Research Center, Cleveland, OH, 1991.
4. Wong, W.A.: “Next Generation Stirling Radioisotope Generator,” Advanced RPS Systems Assessment Team (SAT) Working Meeting Presentation, Germantown, MA, September 1, 2005.
5. Tobery, W.; and Wagner, D.: “Application of General Purpose Heat Source Modules to High Power Stirling Radioisotope Generators,” *Proceedings of the Space Technology and Applications International Forum* (STAIF 2006), Albuquerque, NM, February 12–16, 2006.
6. Holliday, E.; and Keiter, D.E.: “Control Electronics for Palm Power 35 W Free-Piston Stirling Engine,” AIAA 3rd International Energy Conversion Engineering Conference, *Paper AIAA 2005–5750*, San Francisco, CA, August 15–18, 2005.
7. Holman, J.P.: “Heat Transfer,” 696 pp., McGraw-Hill, Inc., New York, NY, 1997.

## REPORT DOCUMENTATION PAGE

*Form Approved*  
OMB No. 0704-0188

Public reporting burden for this collection of information is estimated to average 1 hour per response, including the time for reviewing instructions, searching existing data sources, gathering and maintaining the data needed, and completing and reviewing the collection of information. Send comments regarding this burden estimate or any other aspect of this collection of information, including suggestions for reducing this burden, to Washington Headquarters Services, Directorate for Information Operation and Reports, 1215 Jefferson Davis Highway, Suite 1204, Arlington, VA 22202-4302, and to the Office of Management and Budget, Paperwork Reduction Project (0704-0188), Washington, DC 20503

<b>1. AGENCY USE ONLY</b> <i>(Leave Blank)</i>	<b>2. REPORT DATE</b> November 2007	<b>3. REPORT TYPE AND DATES COVERED</b> Technical Memorandum	
<b>4. TITLE AND SUBTITLE</b> Conceptual Trade Study of General Purpose Heat Source Powered Stirling Converter Configurations		<b>5. FUNDING NUMBERS</b>	
<b>6. AUTHORS</b> J.B. Turpin			
<b>7. PERFORMING ORGANIZATION NAME(S) AND ADDRESS(ES)</b> George C. Marshall Space Flight Center Marshall Space Flight Center, AL 35812		<b>8. PERFORMING ORGANIZATION REPORT NUMBER</b>  M-1207	
<b>9. SPONSORING/MONITORING AGENCY NAME(S) AND ADDRESS(ES)</b> National Aeronautics and Space Administration Washington, DC 20546-0001		<b>10. SPONSORING/MONITORING AGENCY REPORT NUMBER</b>  NASA/TM-2007-215132	
<b>11. SUPPLEMENTARY NOTES</b> Prepared by the Nuclear and Advanced Propulsion Development Branch			
<b>12a. DISTRIBUTION/AVAILABILITY STATEMENT</b> Unclassified-Unlimited Subject Category 20 Availability: NASA CASI 301-621-0390		<b>12b. DISTRIBUTION CODE</b>	
<b>13. ABSTRACT</b> <i>(Maximum 200 words)</i> This Technical Manual describes a parametric study of general purpose heat source (GPHS) powered Stirling converter configurations. This study was performed in support of MSFC's efforts to establish the capability to perform non-nuclear system level testing and integration of radioisotope power systems. Six different GPHS stack configurations at a total of three different power levels (80, 250, and 500 W <sub>e</sub> ) were analyzed. The thermal profiles of the integrated GPHS modules (for each configuration) were calculated to determine maximum temperatures for comparison to allowable material limits. Temperature profiles for off-nominal power conditions were also assessed in order to better understand how power demands from the Stirling engine impact the performance of a given configuration.			
<b>14. SUBJECT TERMS</b> General Purpose Heat Source, Stirling converter, Stirling engine, Radioisotope Power Systems (RPS)		<b>15. NUMBER OF PAGES</b> 40	
		<b>16. PRICE CODE</b>	
<b>17. SECURITY CLASSIFICATION OF REPORT</b> Unclassified	<b>18. SECURITY CLASSIFICATION OF THIS PAGE</b> Unclassified	<b>19. SECURITY CLASSIFICATION OF ABSTRACT</b> Unclassified	<b>20. LIMITATION OF ABSTRACT</b> Unlimited



National Aeronautics and

Space Administration

IS20

**George C. Marshall Space Flight Center**

Marshall Space Flight Center, Alabama

35812